PROCEEDINGS OF SCIENCE

Caustic-like Structures in UHECR Flux after Propagation in Turbulent Intergalactic Magnetic Fields and the caused distortions of the image of a source

Konstantin Alexandrovich Dolgikh,[a,*] **A. Korochkin,**[b] **G. Rubtsov,**[c] **D. Semikoz**[d] **and I. Tkachev**[e]

[a] *ORCID 0009-0007-5353-1621*

[b] *Université Libre de Bruxelles, CP225 Boulevard du Triomphe, 1050 Brussels, Belgium*

[c] *ORCID 0000-0002-6106-2673*

[d] *APC, Université Paris Cité, CNRS/IN2P3, CEA/IRFU, Observatoire de Paris, 119 75205 Paris, France*

E-mail: dolgikh.ka15@physics.msu.ru, sashakoroch@gmail.com, rgbeast@yandex.ru, semikoz@gmail.com, tkachev@ms2.inr.ac.ru

UHECR propagation in a turbulent intergalactic magnetic field in the small-angle scattering regime is well understood for propagation distances much larger than the field coherence scale. The diffusion theory doesn't work and unexpected effects may appear for propagation over smaller distances, from a few and up to 10-20 coherence scales. We study the propagation of UHECRs in this regime, which may be relevant for intermediate mass UHECR nuclei and nG scale intergalactic magnetic fields with 1 Mpc coherence scale. We found that the trajectories form a non-trivial caustic-like pattern with strong deviation from isotropy. In this regime we've found different observable cases of distortions of the source energy spectrum and the images of a source. Thus, measurements of the flux, direction and energy spectrum from a source at a given distance will depend on the position of the observer. In the future, these facts may explain Telescope Array observations.

38th International Cosmic Ray Conference (ICRC2023)
26 July - 3 August, 2023
Nagoya, Japan

*Speaker

PoS(ICRC2023)452

1. Introduction

The propagation of cosmic rays in a turbulent magnetic field in the diffusion regime has been studied in detail [1–3]. However, the propagation of Ultra-High Energy Cosmic Rays (UHECR) in the small-angle scattering regime has attracted less attention. This regime is usually considered trivial, and in the absence of a regular field, cosmic rays are expected to simply form a blurred image of the source if it is at a distance much greater than the coherence length $D \gg \lambda_C$. The average distribution of UHECRs around their sources in this case was obtained in Ref.[4].

Non-trivial lensing effects during UHECR propagation in the Galactic magnetic field were discovered in Ref.[5, 6]. In particular, in Ref. [6] these effects were studied for the case of initially parallel cosmic rays passing through a turbulent magnetic field of the Galaxy. Similar lensing effects for a magnetic field in a cluster of galaxies were studied in Ref. [7].

In this paper, we investigate the propagation of UHECRs from their sources in a certain range of parameters of the intergalactic magnetic field (IMF). It is shown that even in the $D \gg \lambda_C$ regime, the outcome of UHECR propagation is not isotropic, and depending on the position of the observer, the source fluxes can significantly deviate from their average values.

2. Numerical methods

We use publicly available codes `CRbeam` [8] and `CRPropa` [9, 10] for cosmic ray propagation. All interactions and cosmological expansion of the Universe are turned off. The particles were emitted isotropically and propagated until they reached a sphere of a given radius D. For each particle, we store its initial direction, final direction, and final position on the sphere. The resulting output is processed with the package `healpy` [11, 12].

The use of two codes makes it possible to model a turbulent magnetic field in two different ways. In `CRbeam` the magnetic field is generated as a sum of plane waves with random phases and directions [13] and its exact value is recalculated on the fly before each next step during particle propagation. In `CRPropa`, on the contrary, the field is precalculated on the grid and its value is set by interpolation between grid points. In both codes, we generate a magnetic field with a Kolmogorov spectrum and a minimum scale 100 times smaller than the maximum scale.

In all our simulations, `CRbeam` and `CRPropa` produced consistent results. Given the fact that the generation of magnetic fields and the propagation of particles in these codes are carried out in completely different ways, this increases the reliability of the results.

3. Deflection angles of UHECRs in turbulent IGMF

Deflection of cosmic rays in a turbulent field with coherence length λ_C as a function of distance has three regimes. At $D < \lambda_C$, the deflection occurs across the main direction of the magnetic field in the given region. As a result, the deflection grows almost linearly $\theta = (D/D_0)^\alpha$ with $\alpha = 0.9$ in our case. For $D > 5\lambda_C$ deflections occur in diffuse regime and a typical power law corresponds to $\alpha = 0.5$. Finally, in the intermediate regime $\lambda_C < D < 5\lambda_C$, the exponent α is interpolated between the above values.

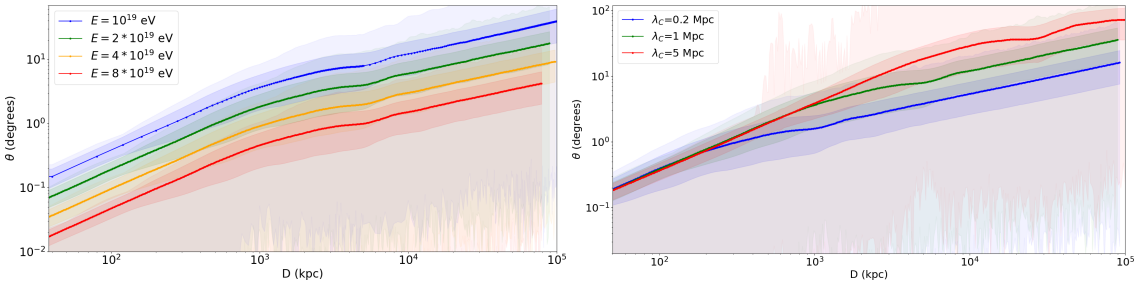

Figure 1: Left panel: Average deflection angle of UHECR protons from the initial direction as a function of distance from the source for $\lambda_C = 1$ Mpc and $B = 1$ nG and several UHECR energies $E = 10, 20, 40, 80$ EeV. Semitransparent filling denotes min-max and standard deviations of deflection angles. Right panel: Average deflection angle of UHECR protons from the initial direction as a function of distance from the source for $E = 10$ EeV and $B = 1$ nG and several coherent lengths $\lambda_C = 0.2, 1, 5$ Mpc.

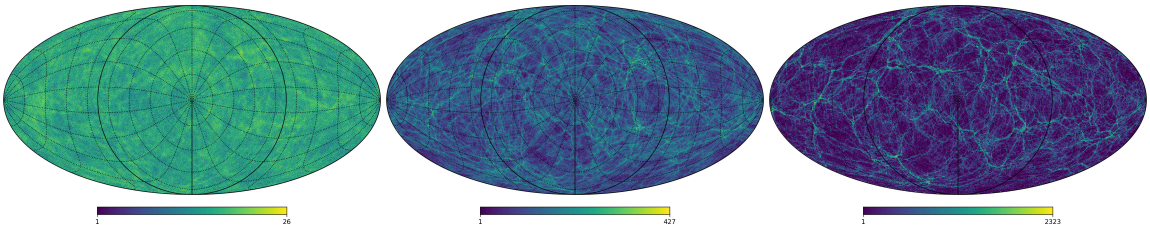

Figure 2: UHECR distribution on a sphere with a radius of 10 Mpc. The magnetic field was turned off after 1,3,10 correlation lengths for panels from left to right, respectively. We see that the global structure is created after the passage of the first 2-3 correlation lengths, then it simply sharpens and intensifies.

Therefore, for $D \gg \lambda_C$ and small deflection angles, we numerically expect

$$\theta \sim 4^\circ \, Z \frac{B}{\text{nG}} \, \frac{10 \text{ EeV}}{E} \sqrt{\frac{D}{\text{Mpc}}} \sqrt{\frac{\lambda_C}{\text{Mpc}}} \tag{1}$$

where Z is the atomic number of the primary particle.

The distance dependence of the proton deflection angle in the other two regimes is shown in Fig. 1, left panel, for $\lambda_C = 1$ Mpc and $B = 1$ nG and several UHECR energies. As expected, an increase in energy reduces the scattering angle. The average deflection angle on the sphere is inversely proportional to the particle energy at all distances to the source, including the intermediate regime $D \sim \lambda_C$.

Similarly, the dependence on the coherence length λ_C is shown in Fig. 1, right panel, for $E = 10$ EeV and $B = 1$ nG. Blue, green and red lines show the mean deflection for $\lambda_C = 0.2$ Mpc, $\lambda_C = 1$ Mpc and $\lambda_C = 5$ Mpc respectively. For greater distances $D \gg \lambda_C$, deflections obey the equation 1.

Relations for mean deflections of cosmic rays presented in this section are well known, however, averaging can erase important properties of UHECR propagation at a given distance from the source. In the next section, we discuss the two-dimensional UHECR flux distribution on the sphere around the source and its dependence on the parameters of the turbulent magnetic field.

In Fig. 2 we show a sky map with UHECR density at a fixed radius of the sphere around the source. This figure shows an example of a UHECR with $E = 10$ EeV propagating in a turbulent magnetic field with strength $B = 1$ nG and coherence scale $\lambda_C = 1$ Mpc. With such a field and

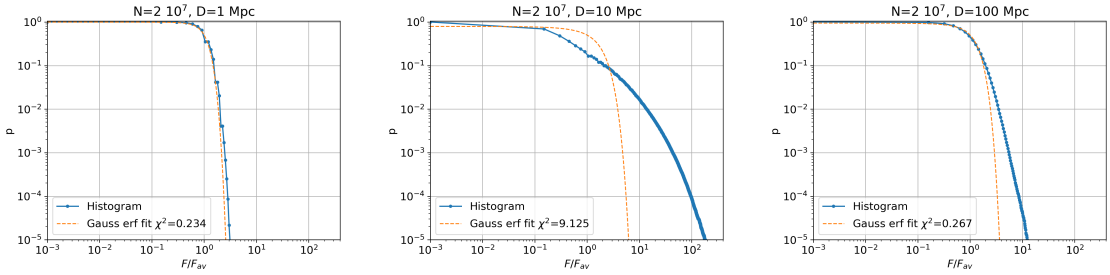

Figure 3: The cumulative probability of arrival with a flux above a given value in units of the average flux on the sphere for an observer located at a distance of 1 Mpc (left panel), 10 Mpc (middle panel) and 100 Mpc (right panel) from the source. At the distance close to Larmor radius the distribution is strongly non-Gaussian.

energy of cosmic rays, we expect that the maximum anisotropy in the UHECR distribution will be reached at 10 correlation lengths, i.e. at a distance of $D = 10$ Mpc. This distance to the source corresponds to the right panel. The bar under the figure shows the color correspondence to the density of cosmic rays in the structures. Three types of structures can be identified: knots with the highest density, filaments and voids with the lowest density. Note that the typical size of a magnetic field domain with $\lambda_C = 1$ Mpc has an angular scale of 6-10 degrees on this map and corresponds to small features. However, the most prominent and highly visible are the medium-scale structures, with a typical scale of about 60 degrees. To understand the angular scale of these structures, we have shown in Fig. 2 the UHECR density at $D = 10$ Mpc, but when the magnetic field is set to zero outside the 1 and 3 Mpc spheres, see left and middle panels respectively. It can be seen that most of the global structure observed at a distance of 10 Mpc is formed during the passage of the first 3 correlation lengths from the source, its physical size corresponded to the correlation length at that time. Later on the structure mainly sharpens.

It is clear that the observer stands only at one given point on the sphere. By randomly changing its location, we calculate the cumulative probability of observing a flux with an intensity higher than a given value, which is shown in the Fig. 3. The x-axis is normalized to the mean density on the sphere. We plot the cumulative probability at a distance of 1, 10, and 100 Mpc from the source, from the left panel to the bottom, respectively for $\lambda_C = 1$ Mpc, $B = 1$ nG, and $E = 10$ EeV. Both at small and large distances, the probability distribution is similar to Gaussian. However, in the middle panel it is very far from Gaussian. The probability of getting a flux below average is 80%. At this distance from the source, the initial flux is likely to decrease, e.g. by a factor of 10 with a probability of about 20%. The probability of an order of magnitude gain is only 2% .

4. UHECR source image

We studied images of UHECR sources for experimental applications. First of all we research a flux amplification in knots and filaments and flux deficit in a voids depends on energy and distance. In Fig. 4 we placed spherical observes with $R = 100kpc$ in a knot and $R = 1Mpc$ in a void and explored flux depends on energy. The y-axis is normalized to the mean flux on the sphere. Both lines converge smoothly to unity with increasing energy.

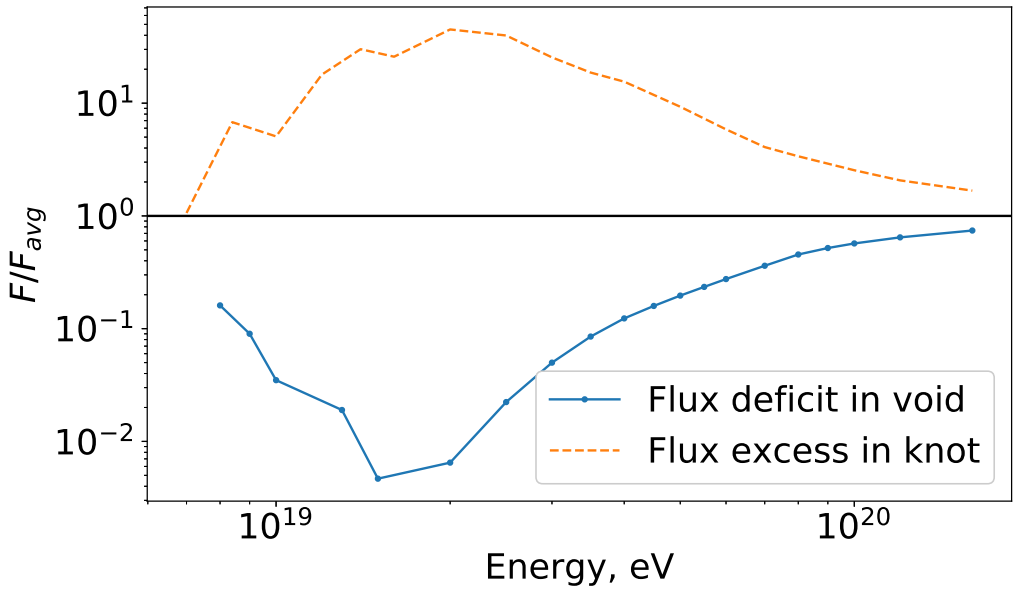

Figure 4: Example of a flux depends on energy in knot at $D = 20$ Mpc and $E = 2 * 10^{19}$ eV and void at $D = 30$ Mpc and $E = 1.5 * 10^19$ eV, magnetic field $B = 1$ nG in both cases.

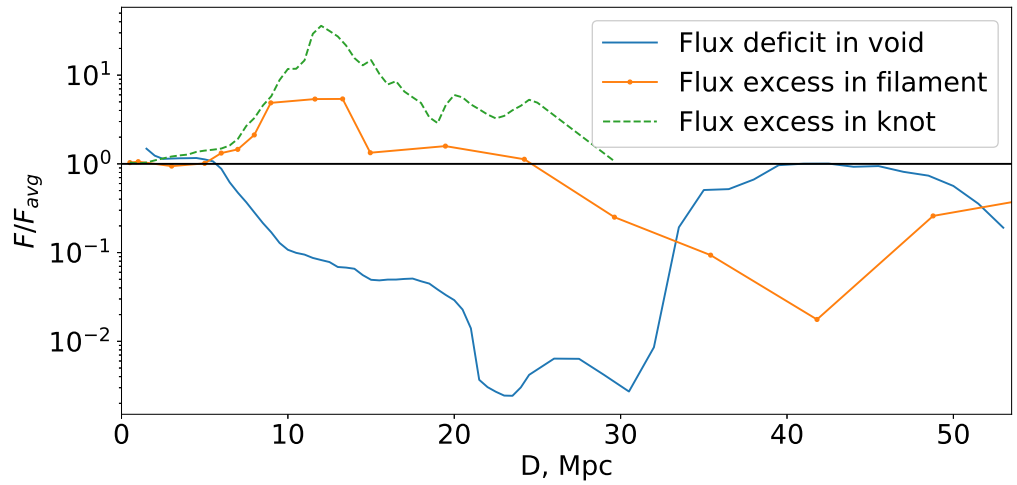

Figure 5: Example of a fluxes excess or deficit in a knot, filament and void at $E = 10$ EeV, $B = 1$ nG at different distances.

In Fig. 5 we placed spherical observes with $R = 100kpc$ in a knot and filament and $R = 1Mpc$ in a void and explored flux depends on distance to the source. The y-axis is normalized to the mean flux on the sphere.

As you can see the flux in the void could be in hundreds of times less than the average. Against in knot or filament we can see flux amplification in dozens of times.

We have studied some cases of observer location 6: observer in a void , observer in a filament, observer in knot. The most likely case is void and in this case we see the source as pale smeared shifted spot. The flux in this case is extremely small and hard for detection. Knot case produces a

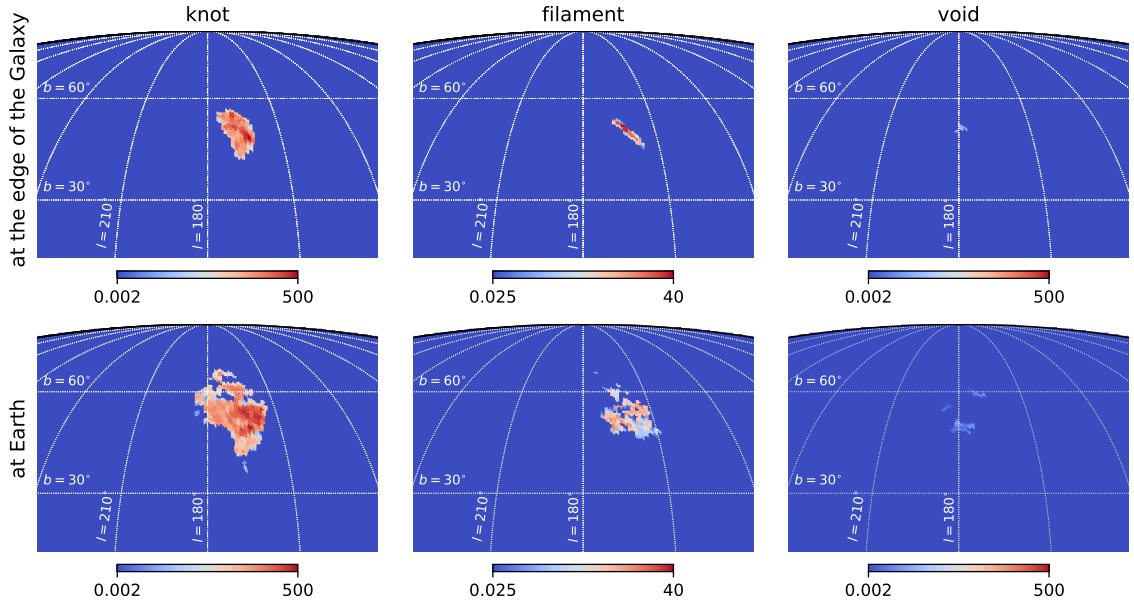

Figure 6: Source images seen by the observer located at knot, filament and void calculated at the edge of the Galaxy and after propagation through the GMF. Color encodes relative amplification of the flux in the pixel compared to the flux expected from the source without focusing effects of IGMF whose image was stretched to the same angular size (in this case all nonzero pixels would have unit amplitude which corresponds to white color on the maps).

bright smudged spot but this case is unlikely too. The most interesting case is the filament, because it has a flow amplification and is not as unlikely as a knot. The source image is very stretched in this case. The stretching disappears when the energy is doubled. After passing the Galaxy magnetic field (GMF), a smeared spot could be formed as in bottom center panel.

5. Conclusions

In this work, we have studied the propagation of UHECRs in a turbulent intergalactic magnetic field in the small-angle scattering regime. We found that even if UHECRs are emitted isotropically from their source, they are distributed anisotropically at a distance of the order of the Larmor radius, and again isotropically at a distance 10 times greater. The enhanced regions merge into a filamentary, caustic-like structure on the sphere. The angular arrangement of these regions is dictated by the structure of the magnetic field at several coherence lengths from the source. The flux coming from the source could be amplified tens of times in knots or weakened hundreds of times in voids. Images of sources in this mode are greatly distorted, which may be important for UHECR observation.

Acknowledgments

Work of K.D., G.R. and I.T. was supported by the Russian Science Foundation grant 22-12-00253. The work of D.S. has been supported by the French National Research Agency (ANR) grant

ANR-19-CE31-0020. Some of the results in this paper have been derived using the healpy and HEALPix packages.

References

[1] F. Casse, M. Lemoine and G. Pelletier, *Transport of cosmic rays in chaotic magnetic fields*, *Phys. Rev. D* **65** (2002) 023002 [astro-ph/0109223].

[2] G. Giacinti, M. Kachelriess and D.V. Semikoz, *Filamentary Diffusion of Cosmic Rays on Small Scales*, *Phys. Rev. Lett.* **108** (2012) 261101 [1204.1271].

[3] G. Giacinti, M. Kachelriess and D.V. Semikoz, *Reconciling cosmic ray diffusion with Galactic magnetic field models*, *JCAP* **07** (2018) 051 [1710.08205].

[4] D. Harari, S. Mollerach and E. Roulet, *Angular distribution of cosmic rays from an individual source in a turbulent magnetic field*, *Phys. Rev. D* **93** (2016) 063002 [1512.08289].

[5] D. Harari, S. Mollerach and E. Roulet, *Magnetic lensing of extremely high-energy cosmic rays in a galactic wind*, *JHEP* **10** (2000) 047 [astro-ph/0005483].

[6] D. Harari, S. Mollerach, E. Roulet and F. Sanchez, *Lensing of ultrahigh-energy cosmic rays in turbulent magnetic fields*, *JHEP* **03** (2002) 045 [astro-ph/0202362].

[7] K. Dolag, M. Kachelrieß and D.V. Semikoz, *UHECR observations and lensing in the magnetic field of the Virgo cluster*, *JCAP* **01** (2009) 033 [0809.5055].

[8] V. Berezinsky and O. Kalashev, *High energy electromagnetic cascades in extragalactic space: physics and features*, *Phys. Rev. D* **94** (2016) 023007 [1603.03989].

[9] R. Alves Batista, A. Dundovic, M. Erdmann, K.-H. Kampert, D. Kuempel, G. Müller et al., *CRPropa 3 - a Public Astrophysical Simulation Framework for Propagating Extraterrestrial Ultra-High Energy Particles*, *JCAP* **05** (2016) 038 [1603.07142].

[10] R. Alves Batista et al., *CRPropa 3.2 — an advanced framework for high-energy particle propagation in extragalactic and galactic spaces*, *JCAP* **09** (2022) 035 [2208.00107].

[11] A. Zonca, L. Singer, D. Lenz, M. Reinecke, C. Rosset, E. Hivon et al., *healpy: equal area pixelization and spherical harmonics transforms for data on the sphere in python*, *Journal of Open Source Software* **4** (2019) 1298.

[12] K.M. Górski, E. Hivon, A.J. Banday, B.D. Wandelt, F.K. Hansen, M. Reinecke et al., *HEALPix: A Framework for High-Resolution Discretization and Fast Analysis of Data Distributed on the Sphere*, **622** (2005) 759 [arXiv:astro-ph/0409513].

[13] J. Giacalone and J.R. Jokipii, *The Transport of Cosmic Rays across a Turbulent Magnetic Field*, **520** (1999) 204.